

Supporting information

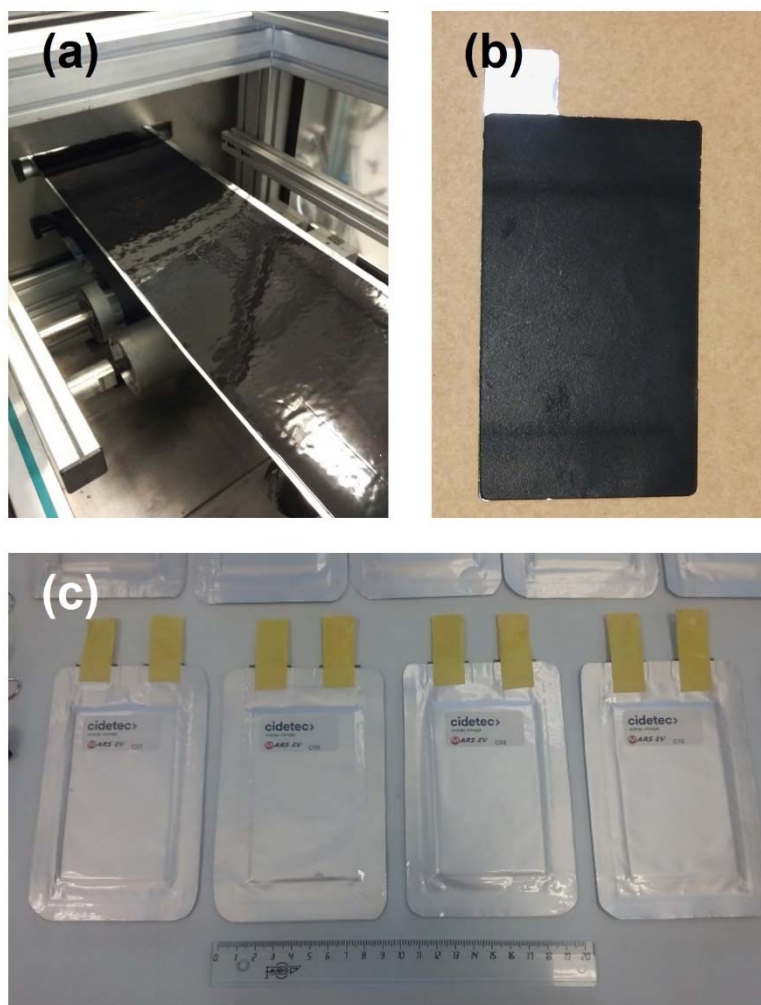


Figure S1. Pictures of (a) the cathode coating after passing through the knife, (b) a cathode, and (c) assembled pouch cells.

Table S1. Testing protocol applied to the LNMO HCCs.

Step	Conditions	Cycles
Charge	$0.2C \rightarrow 5 \text{ V/CV} < 0.05C \text{ \& } 2 \text{ s}$	3
Discharge	$0.2C \rightarrow 3.5 \text{ V}$	
Charge	$0.5C \rightarrow 5 \text{ V /CV} < 0.05C \text{ \& } 2 \text{ s}$	1
Discharge	$0.5C \rightarrow 3.5 \text{ V}$	
Charge	$1C \rightarrow 5 \text{ V/CV} < 0.05C \text{ \& } 2 \text{ s}$	3
Discharge	$1C \rightarrow 3.5 \text{ V}$	
Charge	$0.5C \rightarrow 5 \text{ V/CV} < 0.05C \text{ \& } 2 \text{ s}$	1
Discharge	$0.5C \rightarrow 3.5 \text{ V}$	
Charge	$1C \rightarrow 5 \text{ V/CV} < 0.05C \text{ \& } 2 \text{ s}$	3
Discharge	$2C \rightarrow 3.5 \text{ V}$	
Charge	$0.5C \rightarrow 5 \text{ V/CV} < 0.05C \text{ \& } 2 \text{ s}$	1
Discharge	$0.5C \rightarrow 3.5V$	
Charge	$1C \rightarrow 5 \text{ V/CV} < 0.05C \text{ \& } 2 \text{ s}$	3
Discharge	$5C \rightarrow 3.5 \text{ V}$	
Charge	$0.5C \rightarrow 5 \text{ V/CV} < 0.05C \text{ \& } 2 \text{ s}$	1
Discharge	$0.5C \rightarrow 3.5 \text{ V}$	
Charge	$1C \rightarrow 5 \text{ V/CV} < 0.05C \text{ \& } 2 \text{ s}$	3
Discharge	$8C \rightarrow 3.5 \text{ V}$	
Charge	$0.5C \rightarrow 5 \text{ V/CV} < 0.05C \text{ \& } 2 \text{ s}$	1
Discharge	$0.5C \rightarrow 3.5 \text{ V}$	
Charge	$1C \rightarrow 5 \text{ V/CV} < 0.05C \text{ \& } 2 \text{ s}$	3
Discharge	$10C \rightarrow 3.5 \text{ V}$	
Charge	$0.5C \rightarrow 5 \text{ V/CV} < 0.05C \text{ \& } 2 \text{ s}$	1
Discharge	$0.5C \rightarrow 3.5 \text{ V}$	
Charge	$1C \rightarrow 5 \text{ V/CV} < 0.05C \text{ \& } 2 \text{ s}$	3
Discharge	$1C \rightarrow 3.5 \text{ V}$	

Table S2. Components of the positive electrodes and upper and lower limits defined for the optimization of the slurry.

Component	Weight fraction, wt%	
	Lower limit	Upper limit
LNMO	89	91
Carbon black	4	6
CMC	2	3
Binder	2	3

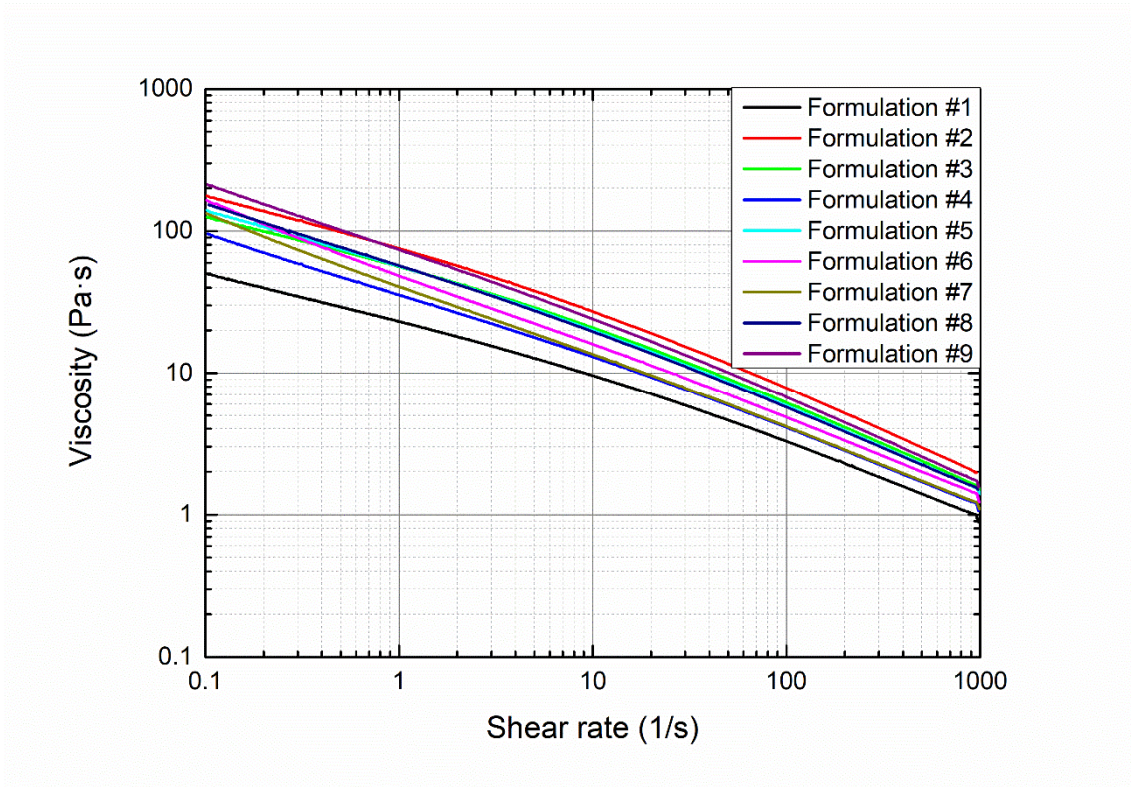


Figure S2. Rheological studies with the different formulations: viscosity vs. shear rate curves.

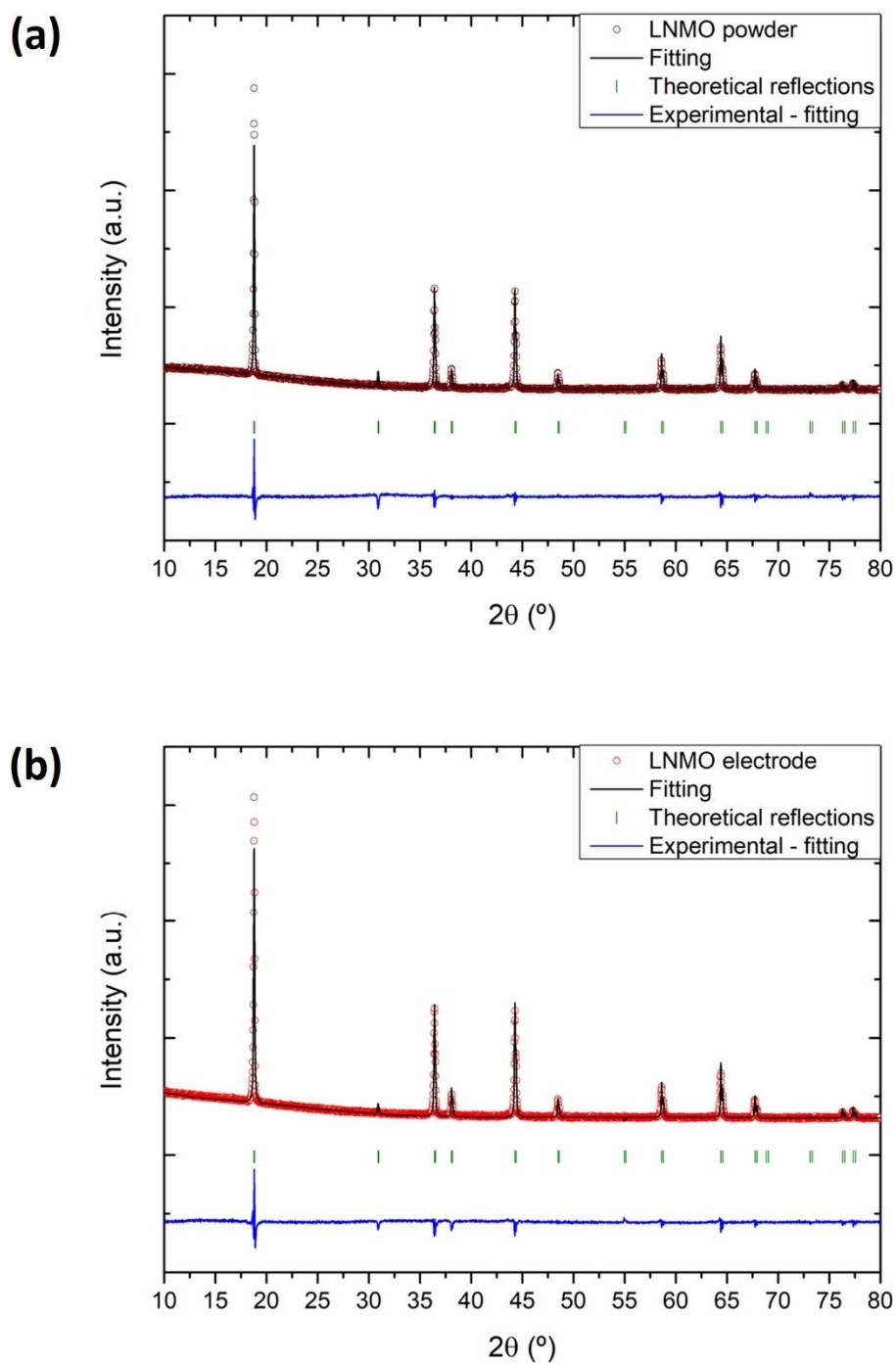


Figure S3. X-ray diffraction patterns of the (a) LNMO powder and (b) a LNMO electrode. Patterns were fitted to LNMO phase using FULLPROF software and its theoretical reflections and the difference between the experimental and the fitting curves are included.

LNMO powder and LNMO electrodes were subjected to XRD analysis. The patterns obtained were fitted using cation-disordered structure with face-centered cubic symmetry (space group $Fd\bar{3}m$). $a = 8.17731$ and 8.17666 Å unit cell parameters were obtained for the LNMO powder and electrode, respectively, evidencing negligible influence of the processing of the material on its crystal structure.

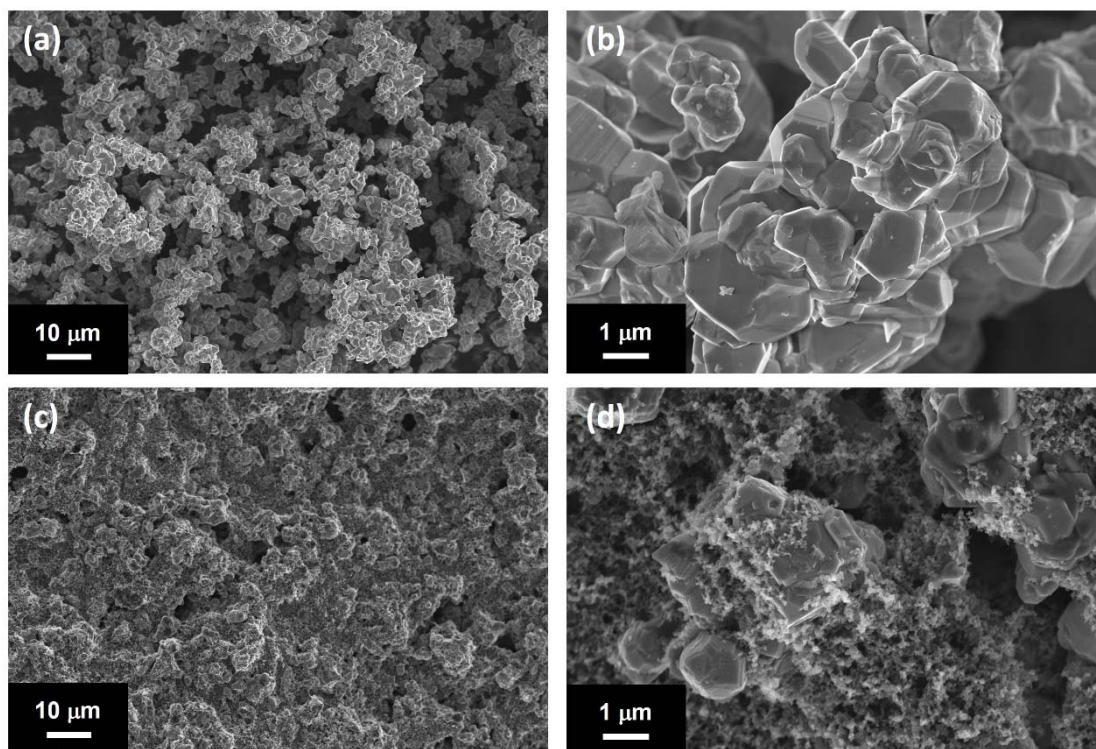


Figure S4. FE-SEM images of the LNMO powder and a LNMO electrode: LNMO powder with magnification (a) X1000 and (b) X10000 and LNMO electrode with magnification (c) X1000 and (d) X10000.

LNMO powder consists of 1-5 μm particle-size clusters (**Figures S4a** and **S4b**). After processing, carbon black appears covering all the electrode surface (**Figure S4c**), generating an electron-conductive matrix to overcome the insulating nature of LNMO. Nevertheless, a closer look to the electrodes (**Figure S4d**) showed that the original LNMO morphology is kept behind the carbon black matrix. No agglomerates were found in the SEM inspection.

Table S3. Functional relations between the concentration of the electrode components and the experimental outputs.

Equation	R ² (%)
$\text{Viscosity} = - 1.73[\text{LNMO}] - 78.19[\text{C65}] - 521.06[\text{CMC}] + 2.24[\text{Binder}] + 1.02[\text{LNMO}][\text{C45}] + 5.98[\text{LNMO}][\text{CMC}] + 0.14[\text{LNMO}][\text{Binder}] + 2.35[\text{C45}][\text{CMC}]$	99.79
$\text{Slope} = - 0.0077[\text{LNMO}] + 0.09[\text{C65}] - 0.96[\text{CMC}] - 1.09[\text{Binder}] + 0.001[\text{LNMO}][\text{C45}] + 0.01[\text{LNMO}][\text{CMC}] + 0.01[\text{LNMO}][\text{Binder}] - 0.02[\text{C45}][\text{CMC}]$	99.57
$\text{Peel strength} = 1.12[\text{LNMO}] + 94.91[\text{C65}] - 1085.85[\text{CMC}] + 438.79[\text{Binder}] - 1.34[\text{LNMO}][\text{C45}] + 11.18[\text{LNMO}][\text{CMC}] - 4.66[\text{LNMO}][\text{Binder}] + 16.95[\text{C45}][\text{CMC}]$	95.64
$0.2\text{C capacity} = 1.11[\text{LNMO}] - 33.55[\text{C65}] - 185.39[\text{CMC}] + 32.48[\text{Binder}] + 0.36[\text{LNMO}][\text{C45}] + 1.95[\text{LNMO}][\text{CMC}] - 0.28[\text{LNMO}][\text{Binder}] + 3.29[\text{C45}][\text{CMC}]$	39.11
$2\text{C capacity} = - 0.38[\text{LNMO}] - 306.02[\text{C65}] - 487.16[\text{CMC}] + 44.40[\text{Binder}] + 3.45[\text{LNMO}][\text{C45}] + 5.09[\text{LNMO}][\text{CMC}] - 0.19[\text{LNMO}][\text{Binder}] + 10.83[\text{C45}][\text{CMC}]$	90.57
$1\text{C capacity} = - 0.59[\text{LNMO}] + 2.95[\text{C65}] - 449.77[\text{CMC}] - 921.56[\text{Binder}] + 0.26[\text{LNMO}][\text{C45}] - 4.60[\text{LNMO}][\text{CMC}] + 10.29[\text{LNMO}][\text{Binder}] - 5.52[\text{C45}][\text{CMC}]$	98.10

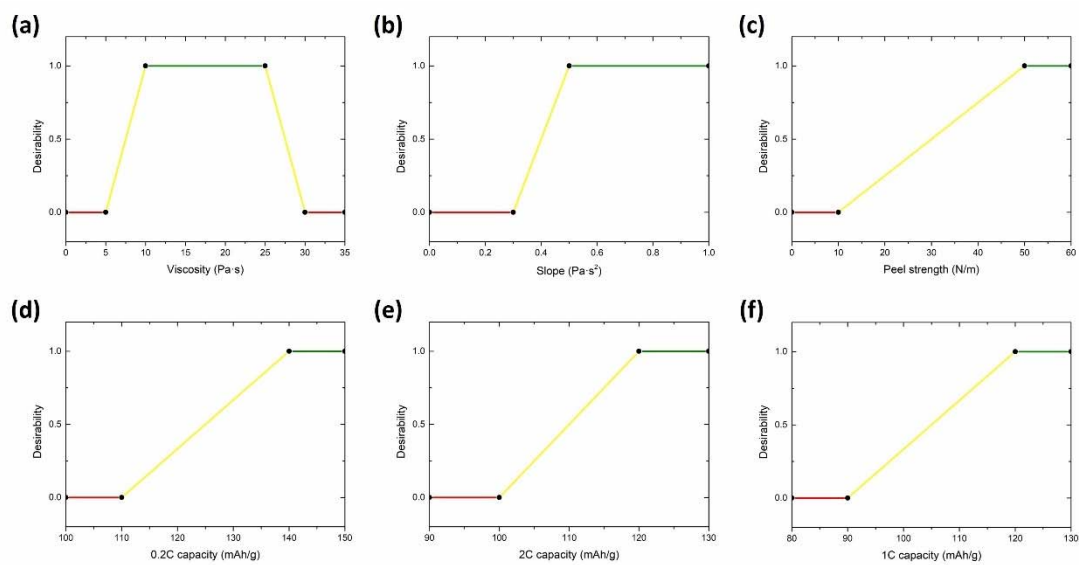


Figure S5. Derringer-Suich desirability functions for the different experimental outputs under evaluation: (a) viscosity, (b) viscosity slope, (c) peel strength, (d) 0.2C capacity, (e) 2C capacity, and (f) 1C capacity.

Table S4. Desirability of the different samples for each parameter, group of parameters and the global desirability.

Formulation	Viscosity at 10 s ⁻¹	Viscosity slope	Peel strength	Feasibility	Specific	Specific	Specific	Electrochemical performance	Global desirability
					capacity at 0.2C	capacity at 2C	capacity at 1C		
1	0.920	0.204	0.670	0.774	0.609	0.823	0.821	0.891	0.928
2	0.572	0.195	0.272	0.647	0.574	0.418	0.613	0.819	0.879
3	1.000	0.105	0.185	0.580	0.601	0.516	0.591	0.834	0.873
4	1.000	0.498	0.372	0.782	0.633	1.000	0.901	0.917	0.939
5	1.000	0.342	0.561	0.801	0.553	0.604	0.246	0.761	0.878
6	1.000	0.893	0.488	0.876	0.531	0.838	0.930	0.883	0.939
7	1.000	0.794	0.864	0.950	0.6	0.855	0.394	0.830	0.926
8	1.000	0.462	0.550	0.827	0.621	0.948	0.668	0.884	0.932
9	1.000	0.639	0.522	0.852	0.643	1.000	0.810	0.910	0.946

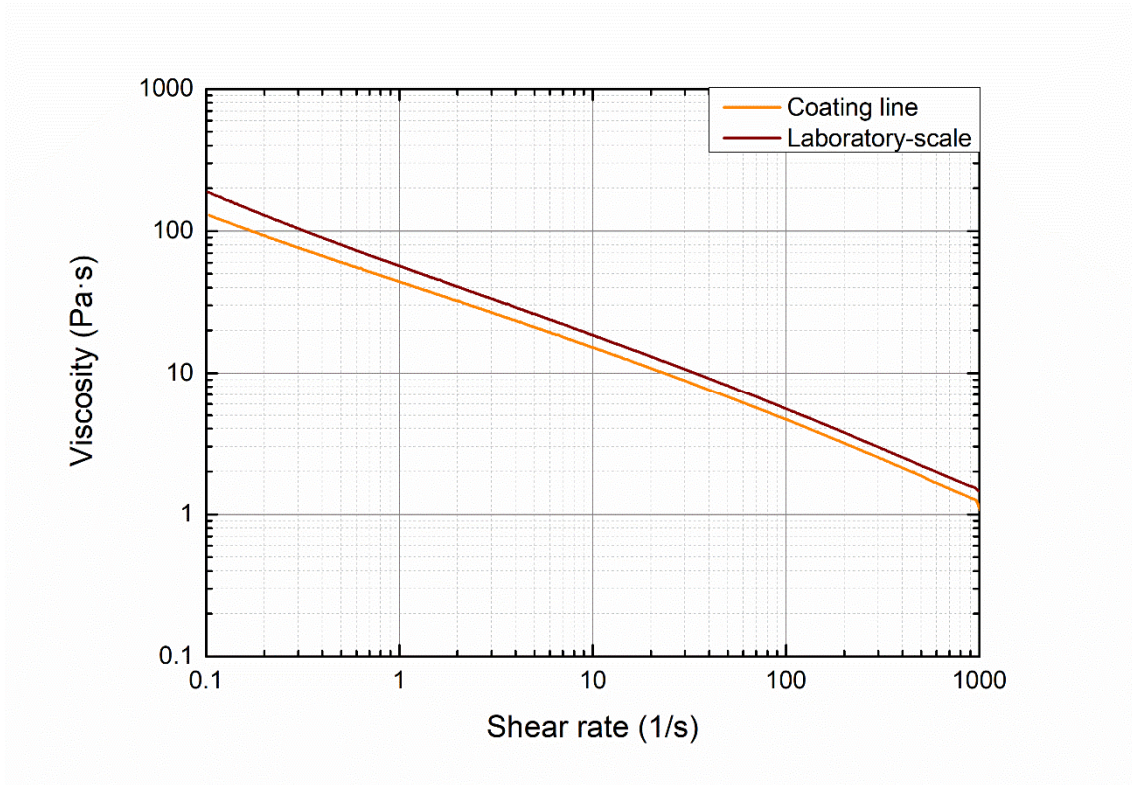


Figure S6. Rheological analyses (viscosity vs. shear rate curves) of the laboratory-scale slurry with formulation #10 and slurry prepared for upscaling to the coating line with the same formulation.

As expected based on the regression coefficient for equation 3 (97.83%), there are slight differences between the global desirability values obtained experimentally and the values obtained with equation 3. Both values for each formulation are compared in **Table S5**.

Table S5. Experimental and mathematical desirability values obtained for the 9 formulations in this study.

Formulation	Experimental D	Mathematical D
1	0.928	0.930
2	0.879	0.882
3	0.873	0.867
4	0.939	0.933
5	0.878	0.884
6	0.939	0.944
7	0.926	0.924
8	0.932	0.943
9	0.946	0.932

Interestingly, the highest experimental and mathematical desirability values are not obtained with the same formulation: the highest mathematical desirability was obtained with formulation #6. These differences are attributed to experimental errors and, thus, it is better to use the mathematical desirability as the referential parameter to evaluate the formulations.

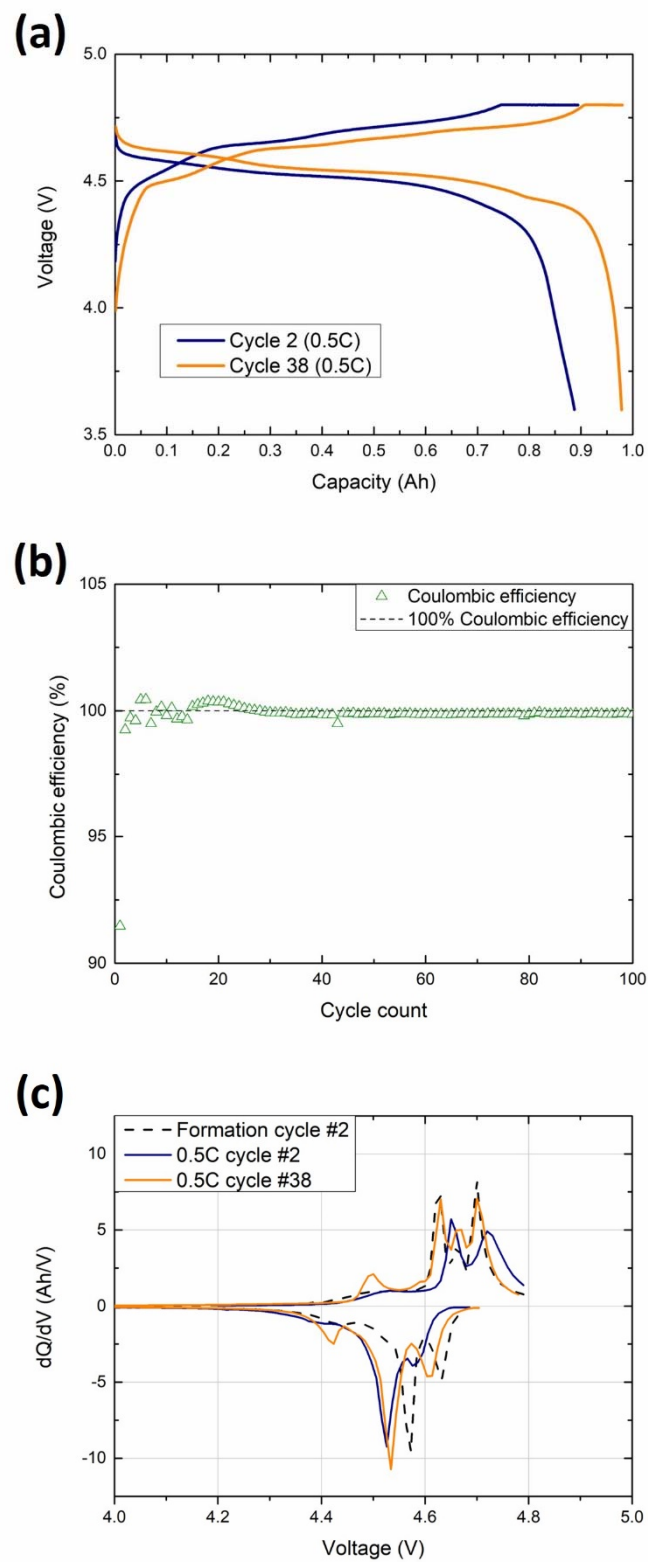


Figure S7. (a) Voltage vs. capacity representation of the 2nd and the 38th cycles with the pouch cells cycled at 0.5C. (b) Coulombic efficiency of the cells subjected to 0.5C C-rate. (c) dQ/dV vs. voltage representation of the 2nd and the 38th cycles with the pouch cells cycled at 0.5C.